Design of Metal Mesh THz Filters Exploiting Adjoint Sensitivity Analysis

Ahmed Y. Elsharabasy, Mohamed H. Bakr, and M. Jamal Deen

Department of Electrical and Computer Engineering
McMaster University, Hamilton, ON L8S 4K1, Canada
elsharay@mcmaster.ca, mbakr@mcmaster.ca, jamal@mcmaster.ca

Abstract ─ We introduce a novel approach for tuning the bandwidth of metal mesh THz filters. Our approach utilizes the adjoint sensitivity with respect to user-defined shape control parameters. Derivative-based optimization is exploited to evolve the initial template of the filter to a new design which satisfies the design specifications. We suggest a smoothing step for the sharp metallic edges that can be implemented in the final structure. Examples are presented to illustrate the efficiency of the technique in tuning the filter's bandwidth.

Index Terms ─ Adjoint sensitivity, derivative-based optimization, frequency selective surfaces, metal mesh filters, simulation, terahertz filter.

I. INTRODUCTION

The Terahertz (THz) frequency range has recently attracted the attention of many researchers [1-10] because it can be used for many applications such as space-based astronomy [2], biotechnology [3], THz spectroscopy [4], imaging [5-6], materials' research [7], security for military and civil applications [8], and sensing [9]. In addition, greater bandwidths are expected from wireless communication systems operating in the THz range. Such systems would require new types of filters. This is one of the motivations for the current research on filter designs that operate in frequency bands from hundreds of GHz to few THz [10].

THz bandpass filters (BPFs) [11-12] are used to eliminate out of band radiation reaching the detector or limit the radiation from a broadband source. In addition, a BPF can be used to improve the signal-to-noise ratio for better detection and measurement by blocking out-of-band thermal radiation. Terahertz BPFs may be classified into three main types; absorption filters [13], multilayer dielectric filters [14], and metal mesh filters [11]. The cross absent filter (CAF) is one of the most successful metal mesh bandpass filters because of its simple design and manufacturability. The CAF filter's response is determined by the geometrical dimensions of each cell, i.e. the arm length and width. Previous studies [11,15-16] succeeded in adjusting the filter response by tuning these geometrical parameters, in addition to the periodicity [17].

The previous approaches in [11,17] had limitations in improving the performance of the filter. Tuning was carried out with the cross arm length and width, and the periodicity. To improve further the performance of CAF bandpass filters, we introduce a derivative-based optimization algorithm that is capable of evolving the filter geometry by exploiting the well-studied adjoint sensitivity technique [18-20]. Our optimization approach exploits more geometrical variables thus enabling more degrees of freedom to improve the performance. The sensitivities are estimated using only one EM simulation regardless of the number of designable parameters. In our approach, the finite element electromagnetic solver ANSYS HFSS [21] is driven by a MATLAB optimization algorithm to change the bandwidth of the filter while maintaining the same centre frequency.

II. OPTIMIZATION PROBLEM

The optical performance, i.e. the transmission of the filter, is a function of the parameters of the filter geometry. Therefore, an efficient optimization algorithm is required to get the optimal parameters that achieve the desired performance.

A. Objective function

The addressed design problem can be put in the following mathematical form:

$$\min_{\boldsymbol{x}} F(\omega, \boldsymbol{x}), \tag{1}$$

$$\text{subject to: } \boldsymbol{g}(\boldsymbol{x}) \le 0. \tag{2}$$

where $F(\omega, \boldsymbol{x})$ is the objective function (e.g., magnitude of the *S*-parameters) to be minimized over the desired frequency range and $\boldsymbol{x} \in \mathbb{R}^n$ is the vector of designable parameters. This objective function includes all the design specifications over different frequency bands. The vector $\boldsymbol{g}(\boldsymbol{x})$ represents the linear and nonlinear constraints.

B. Adjoint sensitivities

The sensitivities of the *S*-parameters with respect to all design parameters can be obtained at minimal extra

Submitted On: June 19, 2018
Accepted On: May 12, 2019

computational cost exploiting adjoint sensitivities. The original simulation supplies the S-parameters and their sensitivities with respect to all parameters. This technique is known as self-adjoint sensitivity analysis (SASA) [18]. Variations of this approach are available in a number of commercial EM solvers (e.g., ANSYS HFSS).

In the frequency domain, the objective function is formulated as a complex function $F(\boldsymbol{x}, \boldsymbol{E})$ where $\boldsymbol{E}$ is the vector of electric fields in the frequency domain. $\boldsymbol{E}$ is the solution of the linear system of equations representing a frequency domain method with the system matrix $\boldsymbol{Z}$ and the known excitation vector $\boldsymbol{Q}$ [19]:

$$\boldsymbol{ZE} = \boldsymbol{Q}. \tag{3}$$

By computing the original $\boldsymbol{E}$ and the adjoint $\tilde{\boldsymbol{E}}$ fields, the sensitivities of the objective function with respect to the jth parameter are given by [19]:

$$\partial F / \partial x_j = \tilde{\boldsymbol{E}}^T \left(\left(\partial \boldsymbol{Q} / \partial x_j \right) - \left(\partial \left(\boldsymbol{Z}\bar{\boldsymbol{E}} \right) / \partial x_j \right) \right), \ \forall j \tag{4}$$

where $\bar{\boldsymbol{E}}$ is the solution of (3) at the current set of parameters. Estimating (4) for all parameters requires only the original and adjoint field information. The derivatives of the system matrix with respect to all parameters are already available through the utilized frequency domain solver.

III. METHODOLOGY

The metal mesh filter design in the THz range consists of a frequency selective surface (FSS) with a repeated pattern of fixed template. In our work, the pattern template shown in Fig. 1, is evolved during each step. This creates new filter templates that is more likely to satisfy the required design specifications. For a metal mesh filter with fixed thickness, the filter is divided into four two-dimensional symmetrical quarters allowing each quarter to evolve according to the optimization algorithm. N control points are selected on each quarter including one point on the horizontal x-axis and another one on the vertical y-axis. The origin is considered the centre of the filter template with constant coordinates. It follows that for N control points, we have $(2N\text{-}2)$ design parameters in addition to the length of the unit cell of the array G. This results in $(2N\text{-}1)$ design parameters. The vector of design parameters $\boldsymbol{x} = \left[x_1, x_2, y_2, x_3, y_3, \ldots, x_{N-2}, y_{N-2}, y_{N-1}, G \right]^T$ is shown in Fig. 2. The initial values of these points are set and passed to the EM simulator HFSS. HFSS then simulates the structure and returns both the S-parameters at the selected frequencies and their adjoint sensitivities with respect to all the design parameters. These sensitivities represent the gradient to be utilized within the optimization algorithm. A custom script is used to control HFSS and allow the MATLAB optimizer to drive the EM simulator. The built-in constrained optimization algorithm in MATLAB, which is derivative-based optimization, is utilized to reach the optimal set of design variables satisfying the design specifications.

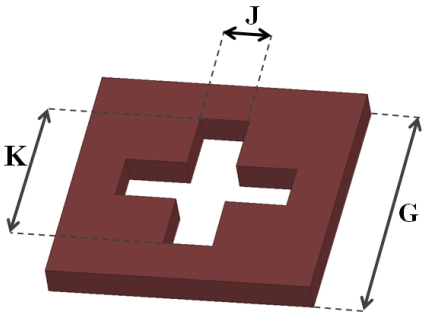

Fig. 1. The main dimensions of a one cell of a cross-absent metal mesh filter.

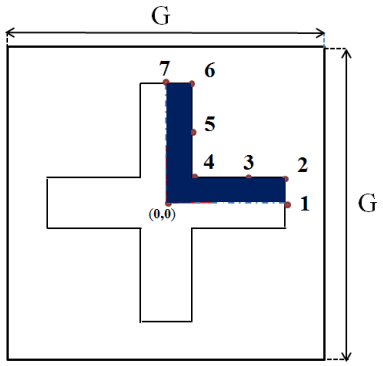

Fig. 2. The control points (1, 2…, 7) with control variables (x_1, x_2, y_2... , y_7, G) that enable the optimizer to evolve the filter template.

Following this procedure, the shape of the filter evolves to a completely different one from the initial template. In some cases, the optimal design may include some sharp edges which could make the filter design too lossy or unrealistic. In our work, we added a smoothing approach as a final step so that design template is smoothed.

IV. EXAMPLES

In our examples, we utilize a cross absent filter (CAF) with initial template parameters from [11,17] and a 12 μm thick copper grid operating at 2.1 THz. We are interested in controlling the bandwidth of this filter. We use one quarter of the filter due to its symmetry. Seven vertices are selected resulting in a total number of parameters of 13 after the length of the unit cell is included ($\boldsymbol{x} \in \mathbb{R}^n$, n=13). COMSOL Multiphysics [22] is used to verify the simulation results obtained using HFSS for the initial filter template. Good matching is achieved confirming the accuracy of our simulations.

First, we consider the case where our target is to widen the bandwidth of the initial bandpass filter while keeping the same resonant frequency. The objective function is the transmittance $|S_{21}|^2$of the BPF which is to be maximized over the frequency range from 1.4 THz

to 2.6 THz. Assuming that the response is symmetrical around the centre (resonant) frequency of 2.1 THz, the optimization problem is given by:

$$\max_{x} \min_{i} \left\{ \left| S_{21}(f_i, \boldsymbol{x}) \right|^2 \right\}, \quad (5)$$

$$\text{subject to} \quad \boldsymbol{x}_l \le \boldsymbol{x} \le \boldsymbol{x}_u,$$

where, $1.4\text{THz} \le f_i \le 2.6\text{THz}$, $i = 1, 2, \ldots, 26$.

To increase the bandwidth of the filter response, we have to maximize the minimum of the transmittance over the defined frequency range. EM simulations are carried out for 26 linearly distributed frequency points over the bandwidth 1.4 THz to 2.6 THz. $\boldsymbol{x}_l$ and $\boldsymbol{x}_u$ are the lower and upper bound constraints preventing the evolution to an unrealizable design. The minimax optimizer starting from the initial point $\boldsymbol{x}_0$ drives HFSS to calculate the S-parameters and sensitivities. These steps are repeated until the predetermined stopping criteria achieved. Following this procedure, we obtain the optimal parameters values $\boldsymbol{x}_f$ that are listed in Table 1.

Table 1: Initial ($\boldsymbol{x}_0$) and final ($\boldsymbol{x}_f$) values of the control parameters for broader bandwidth filter design template

Parameter	$\boldsymbol{x}_0$ (μm)	$\boldsymbol{x}_f$ (μm)
x_1	36.5	39.4
x_2	10.5	22.5
y_2	36.5	47.0
x_3	10.5	20.2
y_3	24.0	25.6
x_4	10.5	26.8
y_4	10.5	29.2
x_5	24.0	25.6
y_5	10.5	19.7
x_6	36.5	45.7
y_6	10.5	24.8
y_7	36.5	47.0
G	113.0	108.8

Figure 3 (a) shows the final filter template. We then eliminate the sharp edges of the optimal design with two different smoothing approaches according to the position of these sharp edges as illustrated in the Fig. 3 (b). The achieved response in Fig. 4, i.e., the optimal one before smoothing. This results show that the bandwidth has been increased by almost 3 times as compared to the initial design. The smoothed filter templates using the both smoothing approaches (additive and subtractive) are shown in Fig. 5. The smoothing responses are similar to the optimal one as shown in Fig. 6. One advantage arising from the smoothing step is that it maintains the same symmetry of the final template as the original (initial) one. Hence, the optical properties of the filter remain independent of the polarization of the incident wave. The same steps were carried out to achieve a narrower bandwidth template, and it successfully shows the capability to obtain one third of the original bandwidth around the same resonant frequency 2.1 THz.

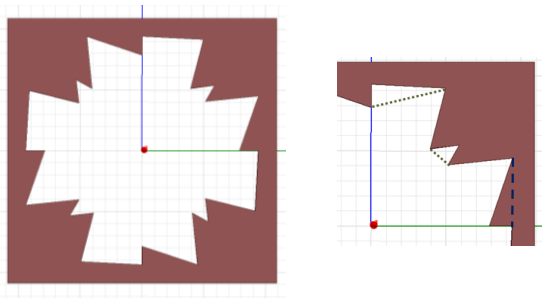

(a) (b)

Fig. 3. (a) A top view of the optimal (final) design for the filter with a wider bandwidth. (b) The smoothing process, the dashed line shows the first subtractive smoothing approach while the dotted line shows the other additive smoothing approach.

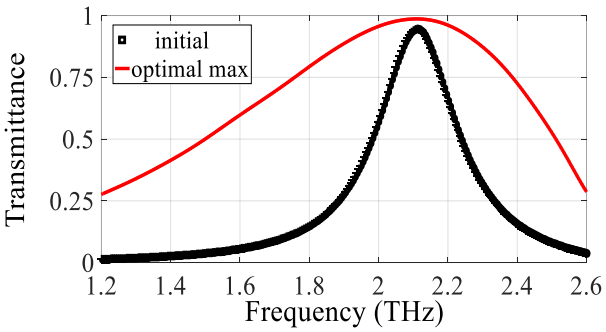

Fig. 4. The transmittance of the initial filter template (…), and of the final (optimal) design (—).

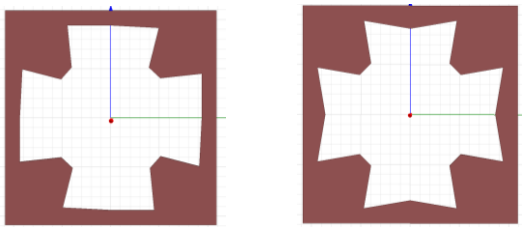

(a) (b)

Fig. 5. A top view of the first smoothed (modified) version of the filter with a wider bandwidth: (a) subtractive smoothed 1, and (b) additive smoothed 2.

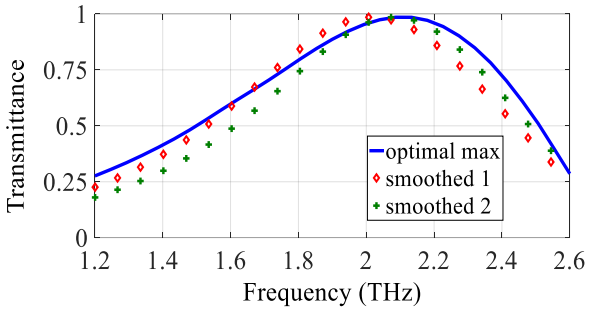

Fig. 6. The transmittance of the optimal filter template (—) and the two smoothed versions for the wide band filter (◊) and (+).

V. CONCLUSION

In this work, we presented an optimization algorithm that exploits efficient adjoint sensitivity analysis to evolve the geometry of the cross-absent metal mesh THz filters. We are able through simulations to increase or decrease the bandwidth by a factor of three. The final (smoothed) design is polarization independent. In addition, it is easy to fabricate and integrate with other THz systems. The presented technique offers a systemic approach for adjusting the bandwidth of the THz filters for different applications.

REFERENCES

[1] P. Siegel, "Terahertz technology," *IEEE Trans. Microwave Theory Tech.*, vol. 50, no. 3, pp. 910-928, 2002

[2] C. Kulesa, "Terahertz spectroscopy for astronomy: From comets to cosmology," *IEEE Trans. Terahertz Science and Technology*, vol. 1, no. 1, pp. 232-240, 2011.

[3] K. Ajito, "Terahertz spectroscopy for pharmaceutical and biomedical applications," *IEEE Trans. Terahertz Science and Technology*, vol. 5, no. 6, pp. 1140-1145, 2015.

[4] B. Gompf and M. Dressel, "THZ-micro-spectroscopy," *IEEE J. Sel. Top. Quantum Electron.*, vol. 14, no. 2, pp. 470-475, 2008.

[5] P. Jepsen, D. Cooke, and M. Koch, "Terahertz spectroscopy and imaging - modern techniques and applications," *Laser & Photonics Rev.*, vol. 5, pp. 124-166, 2011.

[6] M. J. Deen, ed., *Silicon-based Millimeter-wave Technology*, Advances in Imaging and Electron Physics, Academic Press, Amsterdam, vol. 174, 2012.

[7] P. D. Cunningham, *et al.*, "Broadband terahertz characterization of the refractive index and absorption of some important polymeric and organic electro-optic materials," *Journal of Applied Physics*, vol. 109, pp. 043505-1-043505-5, 2011.

[8] N. Palka, *et al.*, "THz spectroscopy and imaging in security applications," *19th International Conference on Microwaves, Radar and Wireless Communications*, vol. 1, pp. 265-270, 2012.

[9] B. Ung, *et al.*, "Terahertz detection of substances for security related purposes," *Proc. SPIE Smart Structures, Devices, and Systems III*, vol. 6414, pp. 1-6, 2006.

[10] S. Koenig, *et al.*, "Wireless sub-THz communication system with high data rate," *Nat. Photonics*, vol. 7, pp. 977-981, 2013.

[11] D. W. Porterfield, *et al.*, "Resonant metal-mesh bandpass filters for the far infrared," *Appl. Opt.*, vol. 33, pp. 6046-6052, 1994.

[12] C. Winnewisser, *et al.*, "Characterization and application of dichroic filters in the 0.1-3-THz region," *IEEE Trans. Microwave Theory Tech.*, vol. 48, pp. 744-749, 2000.

[13] A. J. Gallant, *et al.*, "Terahertz frequency bandpass filters," *Journal of Applied Physics*, vol. 102, pp. 023102-1-023102-5, 2007.

[14] R. Wilk, *et al.* "Highly accurate THz time-domain spectroscopy of multilayer structures," *IEEE J. Sel. Top. Quantum Electron.*, vol. 14, no. 2, pp.392-398, 2008.

[15] Y. Wang, *et al.*, "Micromachined thick mesh filters for millimeter-wave and terahertz applications," *IEEE Trans. Terahertz Science and Technology*, vol. 4, no. 2, pp. 247-253, 2014.

[16] S. A. Alaverdyan, *et al.*, "Development and computer-aided design of metal gratings for microwave mesh polarizers," *IEEE Trans. Microwave Theory Tech.*, vol. 63, no. 8, pp. 2509-2514, 2015.

[17] A. M. Melo, *et al.*, "Metal mesh resonant filters for terahertz frequencies," *Applied Optics*, vol. 47, no. 32, pp. 6064-6069, 2008.

[18] H. Akel and J. P. Webb, "Design sensitivities for scattering-matrix calculation with tetrahedral edge elements," *IEEE Trans. Magn.*, vol. 36, no. 4, pp. 1043-1046, July 2000.

[19] N. K. Nikolova, *et al.*, "Sensitivity analysis of network parameters with electromagnetic frequency-domain simulators," *IEEE Trans. Microwave Theory Tech.*, vol. 54, no. 2, pp. 670-681, 2006.

[20] M. H. Bakr, *Nonlinear Optimization in Electrical Engineering with Applications in Matlab*, IET, 2013.

[21] 'HFSS' ver. 15.0, ANSYS, Inc., Canonsburg, PA, 2014.

[22] 'COMSOL' ver. 5.1, COMSOL Inc., Burlington, MA, 2015.